[^{3}H]OUABAIN AUTORADIOGRAPHY OF FROG RETINA

CHARLES E. STIRLING and ALICE LEE

From the Department of Physiology and Biophysics, School of Medicine, University of Washington, Seattle, Washington 98195

ABSTRACT

The kinetics and distribution of ouabain binding in retinas of *Rana pipiens* were examined quantitatively by scintillation counting and freeze-dry autoradiography. The time-course of binding at several concentrations was consistent with a bimolecular reaction. Estimated equilibrium binding levels gave a Michaelis-Menton relationship with a $K_m = 8.3 \times 10^{-8}$ M and a maximum binding level (B_{max}) = 4.4×10^{-8} mol/g protein. The distribution of binding sites measured autoradiographically varied considerably between layers. The photoreceptor, inner plexiform, and optic nerve fiber layers exhibited the heaviest binding. Within the photoreceptor layer, binding was nonuniform. Binding in the outer segment decreased distally, averaging ~4% of that in the proximal receptor layers ($B_{max} = 4.6 \times 10^{-6}$ M). The origin of the outer segment activity is uncertain at light microscope resolution, as it may be a result of inner segment calyceal processes. Binding within the proximal receptor layers was also nonuniform. Several peaks were observed, with those at the inner segment and synaptic layers being especially noticeable. Assuming an absence of glial cell binding in the proximal receptor layers, we calculated there to be 13×10^6 ouabain or Na^+,K^+ pump sites per rod receptor. Limited measurements suggest a B_{max} of $\sim 8 \times 10^{-6}$ M for the inner plexiform layer.

Measurements of vertebrate photoreceptor currents (19, 44), potentials (3, 7, 41), and Na^+-dependent volume changes (23) are the foundation for the widely held view (17, 18, 32, 40) that there is a continuous flow of positive ions out of the proximal receptor, balanced by an equivalent flow of positive ions into the outer segment. The outward current may result from K^+ diffusing down its electrochemical gradient and possibly from outward electrogenic pumping of Na^+. The outer-segment ionic current is attributed to Na^+ diffusion down its electrochemical gradient through membrane channels. The absorption of light by photopigments located in the outer segment causes the release of a transmitterlike substance (15), possibly Ca^{++} (18), that closes these channels. Consequently, current flow between inner and outer segment is greatest in the dark and is reduced upon exposure to light. Correspondingly, vertebrate photoreceptors (40), unlike their invertebrate counterparts (16), are partially depolarized in the dark and repolarized in light. The ionic gradients supporting these currents are thought to be maintained by Na^+,K^+-ATPase pumps, because the currents are abolished by ouabain (14, 42, 44).

An inner-segment location for the Na^+,K^+ pump has been suggested by Hagins, Penn, and Yoshikami (20, 42) on the basis of their observations of current flow. If the stoichiometry of the pump is 3 Na^+/2 K^+ as reported for squid axons (11) and erythrocytes (29), it is electrogenic and a proximal location would contribute approximately

one-third of the outward current, whereas an outer-segment location would reduce the inward Na^+ current by approximately one-third as compared to a neutral pump.

Biochemical studies of retinal Na^+,K^+-ATPase activity using cell fractionation methods have produced various results. There are claims (6, 13, 21) that outer segments possess a high activity and there are counterclaims (4, 8) suggesting that the reported activities result from contamination with inner segments. Na^+,K^+-ATPase activity in other regions of the retina is unknown. Histochemical studies on the distribution of Na^+,K^+-ATPase in neural tissues are rare (5, 10, 35).

In this study, we have used quantitative light-microscope autoradiography of [^{3}H]ouabain (37) to locate and measure the number of Na^+,K^+ pump sites per photoreceptor and their distribution within the receptor layer.

MATERIALS AND METHODS

Experimental Protocol

Rana pipiens obtained from a local supplier were kept ≤2 wk in a laboratory tank at room temperature. All of the following procedures were carried our under typical laboratory illumination. For the experiments, the animal was decapitated and the head pinned to a corkboard. The lids were cut away and the eye was hemisected at the level of the ora serrata. The retina, with choroid attached, was removed to a dish of 10°C frog Ringer's and dissected into 5-mg wedges. During the dissection, the choroid and most of the pigmented epithelial cells separated from the retina. The wedges were incubated in frog Ringer's containing appropriate concentrations of radiolabeled drugs. After prescribed incubation periods, the tissue was washed in drug-free Ringer's at 0°C for 20–30 min. When autoradiographs were to be prepared, the incubation and wash solutions contained 5% bovine albumin (Matheson, Coleman and Bell, Norwood, Ohio). All solutions were in equilibrium, with 95% O_2 and 5% CO_2.

In the kinetic measurements of ouabain binding using scintillation counting, retina was digested in 0.1 N NaOH overnight and neutralized (HCl) before analysing for total protein (9) and radioactivity (34). [^{3}H]Ouabain and [^{14}C]inulin (New England Nuclear, Boston, Mass) were found to be 98% radiopure by thin-layer chromatography. Ouabain concentration was measured by UV spectrophotometry.

To determine the extent of extracellular washout and to ensure that bound ouabain was not removed by this procedure, we measured the time-course of ouabain and inulin loss at 4°C. Fig. 1 *a* shows the washout curves of retina incubated 20 min in 4×10^{-6} M [^{3}H]ouabain and 0.01% [^{14}C]inulin before transfer to drug-free medium. At the indicated times, the solutions were replaced and analyzed for both isotopes. In one set of experiments, gentle mixing was accomplished by rotation at 15 cycles/min, whereas, in the other set, a more vigorous mixing was accomplished by bubbling, which caused the tissue to tumble rapidly. The bubbling technique, although it gave a slightly faster washout, was abandoned because it removed most of the outer segments. With both mixing conditions, there was a rapid loss of ouabain in the initial 20 min. Thereafter, the tissue content declined slowly toward 50% of its unwashed value. Correspondingly, loss of the extracellular marker inulin was >70 and 85% complete at 20 and 60 min, respectively. The difference between the inulin and ouabain runout curves is attributed to the stable binding of ouabain. These results are in accord with similar studies in other tissues (22, 26, 34).

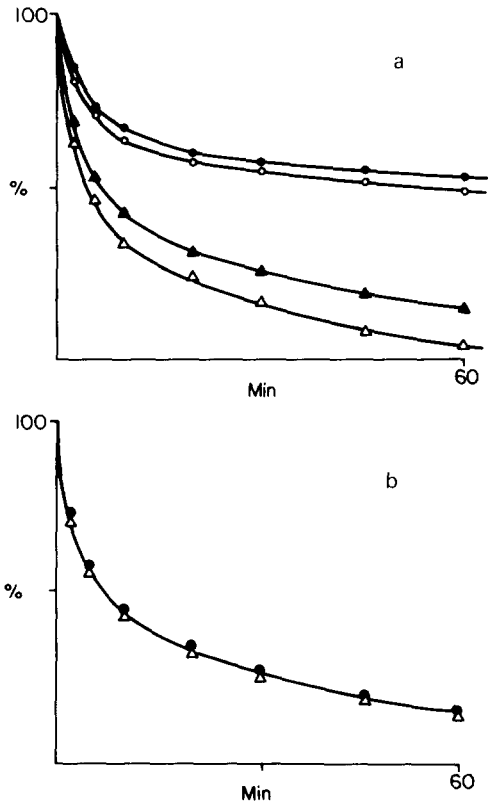

FIGURE 1 Retinal washout kinetics. Ordinates show the fraction of inulin (△, ▲) and ouabain (○, ●) remaining after the indicated periods in drug-free medium at 0°C. Open and closed symbols indicate experiments with and without solution bubbling, respectively. (*a*) Retina was incubated for 20 min in 4×10^{-6} M [^{3}H]ouabain (4 μCi/ml) and 0.01% [^{14}C]inulin (1 μCi/ml). (*b*) Retina was incubated for 20 min in 10^{-4} M [^{3}H]ouabain (4 μCi/ml) and 0.01% [^{14}C]inulin (1 μCi/ml).

In a slightly different set of washout experiments (Fig. 1 *b*), we verified that the difference in inulin and ouabain runout was a result of ouabain binding and that the kinetics of extracellular ouabain loss are the same as those for inulin. We raised the concentration of ouabain to 10^{-4} M while maintaining the radioactivity at the same level as that of Fig. 1 *a*. Under this condition of low specific activity, the ouabain present is primarily extracellular and its runout curve is nearly coincident with that of inulin. The time-course for inulin washout was somewhat slower than that ($t_{1/2}$ < 2 min) reported by Ames and Nesbett (1). We advance no explanation for this disagreement. Methodology and species difference seem to be trivial. The washout kinetics ob-

served here are very similar to those reported by Shaver and Stirling (34) in renal slices (0.5-mm thick).

Autoradiography

After the wash period, tissue was processed for autoradiography as previously described (39). Briefly, frozen tissue was freeze-dried at −40°C under a vacuum of 0.001 torr. The dried tissue was placed in a desiccator, fixed with osmium tetroxide vapor overnight, and then infiltrated in Spurr's low-viscosity embedding medium (Polysciences, Inc., Warrington, Pa.). The tissue blocks were oriented in flat embedding molds and sectioned (1 μm) over water. Sections, on glass slides, were coated with nuclear track emulsion (Kodak NTB 2, Eastman-Kodak, Rochester, N. Y.) by dipping. After drying and various exposures, they were developed (Kodak D-19), fixed and, in some instances, stained (31). Chemography tests produced no evidence of spurious grain production. However, apparent latent image fading over the photoreceptor outer segments was observed occasionally in initial experiments. This was attributed to section rippling, which produces uneven emulsion coating in the photoreceptor region, and/or to incomplete drying of the emulsion. In all of the experiments reported, additional changes of the desiccant were carried out to assure complete drying, and fogged (light-exposed) autoradiographs were included to ensure that neither latent image fading nor rippling had occurred.

The absolute ouabain concentration over a region of the retina was determined by comparing the grain density (grains per square micrometer) with that of the incubation medium. In all experiments, several sections of the incubation medium cut from a sample processed for autoradiography were included on the slide. As a check of the quantitative reliability of the method, a series of standards were prepared from albumin–frog Ringer's containing various concentrations of ouabain and tritium activity. Measurements of these standards are presented in Fig. 2. They show that the grain densities up to 400 grains/1,000 μm^2 are proportional to the concentration of tritium-labeled ouabain.

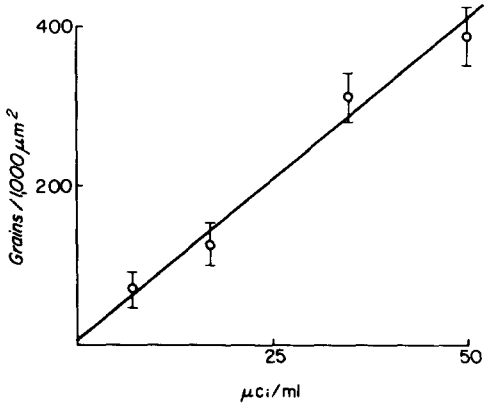

FIGURE 2 Grain-density measurements of incubation media containing the indicated activities of [^{3}H]ouabain. The corresponding ouabain concentrations were 0.8, 2.0, 4.0, and 6.0×10^{-6} M. The grain-density values are the average ± SE of five or more 1,500-μm^2 regions randomly selected from a section. The slope and intercept were determined by linear regression analysis. The autoradiographic exposure time was 15 d.

This standard curve agrees with that published for tritium-labeled galactose and phlorizin (39). For a given level of radioactivity (μCi/ml), grain density also increased linearly with exposure time in the range of 0–400 grains/1,000 μm^2 (measurements not shown).

RESULTS

Kinetics of Binding

To determine the extent of binding-site saturation at a given ouabain concentration and incubation time, we systematically examined the dependence of binding on these parameters. Fig. 3 shows that the initial rate of ouabain uptake increases with concentration. As incubation time increases, the rate of uptake slows and approaches a plateau or equilibrium value at the higher concentrations. Presumably, the lower concentration curves would have reached a plateau had longer incubation times been used. They were not used because the morphology began to deteriorate in retina exposed to ouabain >60 min.

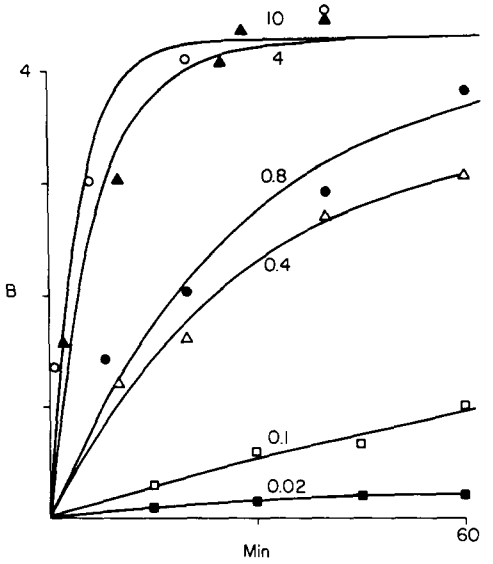

FIGURE 3 Kinetics of [^{3}H]ouabain binding to whole retina. Pieces from six animals were incubated for the indicated times and concentrations. The number above each curve gives the ouabain concentration in micromoles per liter, and *B* refers to ouabain bound in 10^{-8} mol/g of protein. A gram of protein was equivalent to 20 g of wet retina. [^{14}C]Inulin, present in the incubation medium, was used to correct for extracellular ouabain after a 30-min wash in 0°C drug-free Ringer's. Each point is the mean of six measurements. The fractional SD of the fit for a given curve was typically 12%. Error bars were omitted so as not to clutter the diagram.

In a related study (34), ouabain binding to renal tubules exhibited similar properties that were shown to be consistent with a bimolecular reaction. The data of Fig. 3 are also consistent with a bimolecular reaction, as the curves show. They are least squares fit to the bimolecular equation. Details of the method of analysis were published recently in this journal (34). In characterizing glycoside binding, it is desirable to know the maximum binding level (B_{max}) and the equilibrium binding constant (K_m). To obtain these parameters, one needs to know the dependence of ouabain bound at equilibrium (B_∞) on the free concentration ([O]) of ouabain. At the higher concentrations of Fig. 3, the binding reaction is near equilibrium. At the lower concentrations, especially 0.1 and 0.02×10^{-6} M, departure from equilibrium is significant. We assumed that binding at all concentrations was bimolecular and estimated the equilibrium values by extrapolating the curves of Fig. 3 to infinite time (34). Fig. 4 shows a plot of these values as a function of concentration. The values fit the familiar Michaelis-Menton relationship rather well: $B_\infty = B_{max}[[O]/([O] + K_m)]$, where $B_{max} = (4.4 \pm 5) \times 10^{-8}$ mol/g protein and $K_m = (8.3 \pm 1) \times 10^{-8}$ M. These results suggest that ouabain binds to a single high-affinity site of the Na^+,K^+-ATPase with bimolecular kinetics. The absence of a significant linear component of binding, as observed by Mills and colleagues (26) in the frog skin, further suggests that nonspecific binding is negligible.

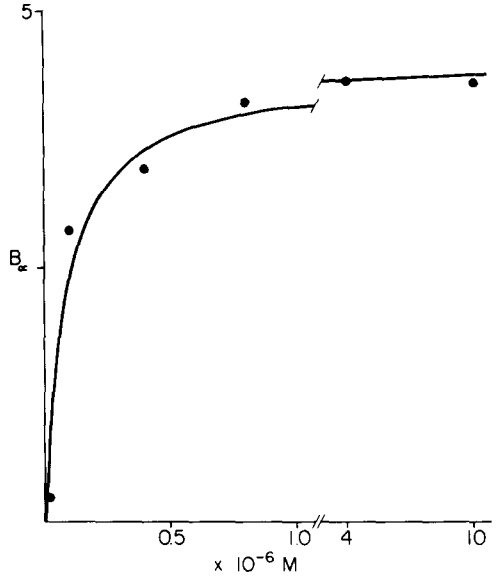

FIGURE 4 Dependence of ouabain bound at equilibrium on concentration. As noted in the text, B_∞ was obtained by extrapolating the curves of Fig. 3 to infinite time. The amount bound, B_∞, is in 10^{-8} mol/g of protein. The curve is a least squares fit using nonlinear methods (see text).

Autoradiography

The distribution of ouabain binding sites in the photoreceptor and inner nuclear layers under saturation conditions is shown in the autoradiograph of Fig. 5. The most striking feature is the difference in grain densities between the outer segment and the remainder of the receptor. An occasional receptor exhibits a region of binding that extends into the outer-segment zone. These may be green rods (arrows) whose inner segments extend beyond the ciliary junctions of the more numerous red rods (27). Within the proximal layers, binding appears to be most dense at the ellipsoid region and the synaptic or outer plexiform layer.

A higher magnification view of receptor binding in another animal is shown in Fig. 6. The difference in grain density between the outer segments and proximal receptor layers is clearly evident. However, the grain density of the first several micrometers of the outer segments is significantly above background levels and appears to decrease distally toward their tips. This impression is supported by grain-density measurements of serial sections (presented in a later section). The grains of the proximal receptor usually are associated with cell boundaries; this is especially evident in the nuclear regions. However, grains are sometimes found over cytoplasmic regions. This probably results from the inclusion of cell membrane in the plane of sectioning, which is to be expected with 1-μm sections of small cells (7-μm Diam) with complex surface folds. The cluster of grains over the proximal receptor are regions of high density as quantitative analyses show (Fig. 11 *a*); they may result from a high cell-membrane surface area in these regions.

Binding density levels decrease sharply as one passes from the receptor layer to the inner nuclear layer (Fig. 5), which is filled principally by cell bodies. As shown in Fig. 7, activity picks up again in the inner plexiform layer, falls again over the ganglion cell bodies, and rises over the optic nerve fibers. Thus, in the nonreceptor layers, the binding activity is the highest in the regions possessing fine processes and synapses.

The specificity of binding was examined by two established methods (30, 36): raising the concen-

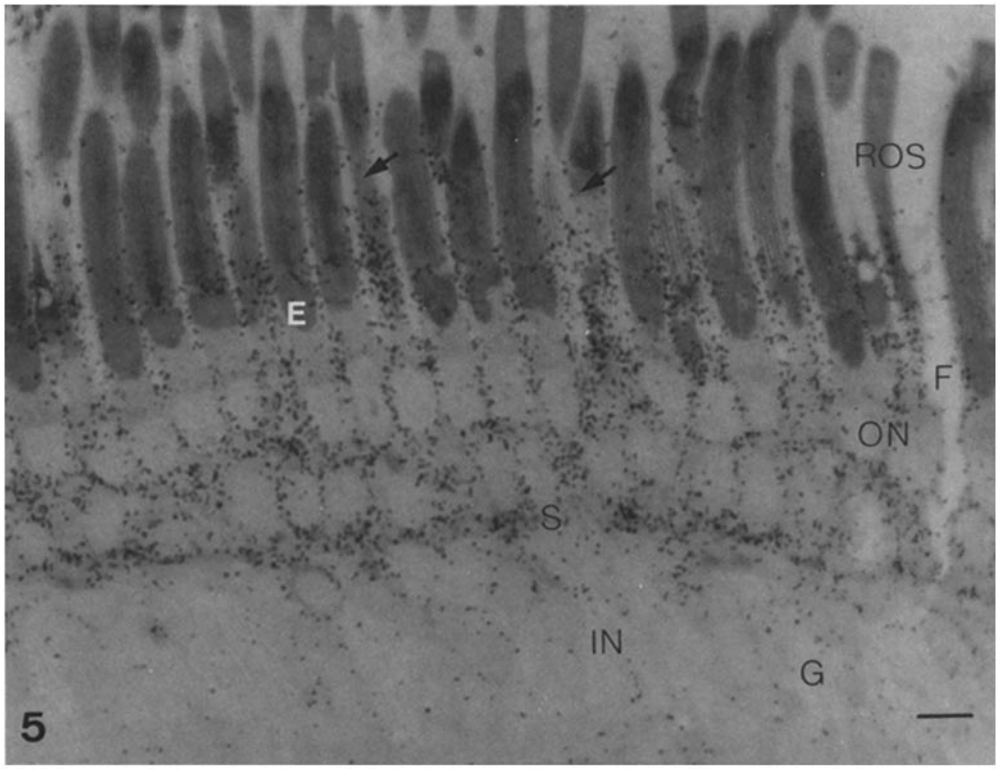

FIGURE 5 Low-magnification autoradiograph of retina incubated for 20 min in 2×10^{-6} M (25 μCi/ml) and washed for 20 min. The preservation of morphology is generally quite good. Rod outer segments (*ROS*) and mitochondria-rich ellipsoids (*E*) are darkly stained by osmium. Frequently, individual outer segments exhibit variation in osmium staining; its cause is not known. Freezing has produced an occasional fracture (*F*) and marked striations in the outer segments; the latter are probably related to the incisures observed (32) with conventional fixation. Other characteristic structures are the double row of nuclei in the outer nuclear layer (*ON*), the outer plexiform and synaptic layers (*S*), and the inner nuclear layer (*IN*) with glial fibers (*G*). Arrows indicate green rods. Exposure, 8 d; bar, 10 μm.

tration of K^+ (Fig. 8) and raising the concentration of ouabain with unlabeled drug (Fig. 9). Increasing the medium K^+ from 2.5 to 50 mM lowered the level of binding by 30% as compared to its control (Fig. 6). Increasing the ouabain concentration by 10^{-3} M, thereby decreasing its specific activity, reduced the grain density to background levels. These control experiments (Figs. 8 and 9) indicate insignificant uptake by both nonspecific binding sites and cellular entry. The absence of radioactivity indicates, as well, that the wash step removed most of the extracellular ouabain from the receptor layer.

Grain-Density Measurements

The number of Na^+ pump sites per rod and their distribution is a problem of considerable interest. To answer the question, we applied grain-density analyses to autoradiographs similar to those presented. First, we established that the kinetics of binding to photoreceptors did not differ significantly from those observed for the whole retina. Pieces of retina from a single animal were incubated in high specific activity [^{3}H]ouabain at the concentrations and for the times shown in Fig. 10 (see legend for experimental details). The curves were obtained as in Fig. 3. These experiments demonstrate that the kinetics of binding to the receptor layer as measured autoradiographically differ little from those measured in the whole retina by scintillation counting. The initial binding rates are slightly faster in the receptor layer. This is not surprising, because it is more accessible than the interior layers, particularly the inner plexiform

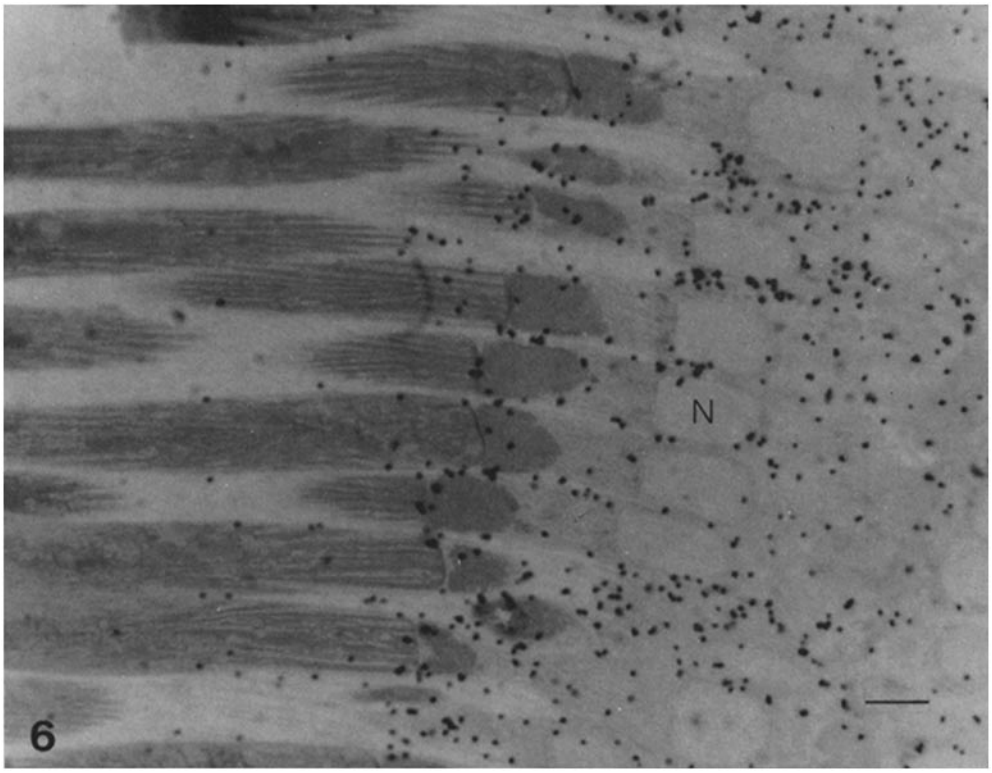

FIGURE 6 High-magnification view of an ouabain autoradiograph prepared from retina incubated for 20 min in 10^{-6} M [^{3}H]ouabain (12.5 μCi/ml) and washed for 20 min. The outer segment striations and ellipsoid bodies stand out clearly at this magnification. The nuclei (*N*) of several red rods are in register. Below the first row of nuclei, the interdigitation of adjacent membranes is so extensive that receptor borders cannot be distinguished. Hence, the pockets of high grain density cannot be assigned to any particular structure. Exposure, 16 d; bar, 5 μm.

layer, which is a major contributor to total retinal binding. The maximum or saturation binding level, estimated from the 10^{-5} M curve for this animal, was 5.1 M ± 0.6 SE. Maximum photoreceptor binding levels in four additional animals averaged 4.6 M ± 0.09 SE. The maximum binding level of the receptor layer is approximately twice that measured in retinal slices,[1] which is reasonable, considering the nonuniformity of binding between layers (Fig. 5).

Receptor Distribution

The measurements shown in Fig. 10 represent the mean binding level for the proximal half of the photoreceptor layer. Earlier, it was suggested that binding within the receptor layer was not uniform. We investigated this important question by analyzing serial sections cut perpendicular to the long axis of the receptor layer. Fig. 11 *a* shows the variation of binding-site density with position along the receptor. Each point is the average of five groups of photoreceptors. Each group contained about 12 cells, which were followed from outer-segment tip to outer plexiform layer. Autoradiographic exposure was longer than usual, to bring out low levels of binding in the distal portions of the outer segment. As can be seen, there is a low level of binding over most of the outer segments that shows a modest increase just before the ciliary junction (35–40 μm). At the ciliary junction, there is a sharp increase followed by two valleys and peaks before the low activity region of the inner nuclear layer. The photoreceptor diagram at the bottom of Fig. 11 *a* indicates the

[1] 20 g of wet retina was equivalent to 1 g of protein. Assuming a retinal density of 1 g/ml, then 10^{-8} mol/g of protein is equivalent to 5×10^{-7} M. Thus, a B_{max} of 4.4×10^{-8} mol/g of protein (Fig. 3) is equivalent to 2.2×10^{-6} M.

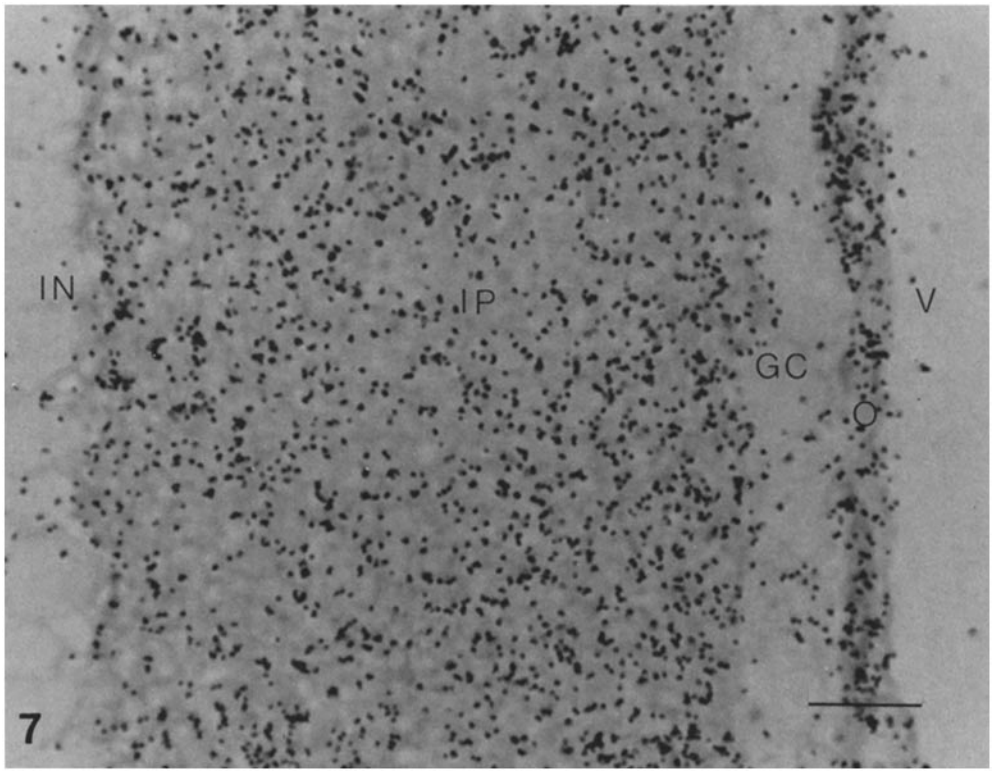

FIGURE 7 High-magnification view of an autoradiograph from proximal retina incubated for 25 min in 2×10^{-6} M [^{3}H]ouabain (25 μCi/ml) and washed for 20 min. The several layers shown are inner nuclear (*IN*), inner plexiform (*IP*), ganglion cell (*GC*), optic nerve fibers (*O*) and vitreous humor (*V*). Exposure, 23 d; bar, 10 μm.

approximate anatomical location of the measurements. The valleys coincide roughly with the nuclear layers and the last peak coincides with the synaptic layer. Representative autoradiographs from selected locations are shown in Fig. 11 *b*.

Inner Plexiform Layer

Autoradiographic measurements of this layer are not complete; however, we present preliminary experiments in Fig. 12 that indicate the maximum level of binding and a problem encountered in measuring the kinetics of binding. At 10^{-5} M, binding proceeded at a rate slightly slower than that presented in Fig. 3 and appproached a plateau value of nearly 8×10^{-6} M in 30 min. However, binding at the lower concentrations proceeded at a much slower rate than those in Fig. 3. Binding to the photoreceptor layer at the lower concentrations in these experiments was similar to that in Fig. 10.

This behavior, typical photoreceptor binding accompanied by low inner plexiform layer binding at low doses of ouabain, was noted occasionally in other autoradiographic experiments. In all of these experiments, we noted that the retina had folded, thereby constricting diffusional access to the inner layers via the vitreous pathway. A possible explanation for this phenomenon is that photoreceptor binding at low concentrations significantly reduced the amount of ouabain reaching the more proximal layers, thereby slowing their rate of binding. At higher concentrations (10^{-5} M), the extraction of ouabain along the diffusional pathway is negligible and binding proceeds at its usual rate. Similar penetration problems with ouabain were observed in avian salt-gland slices (12).

DISCUSSION

The kinetic analysis presented here shows that the characteristics of ouabain binding to the retina are equivalent to those observed in other cellular systems (2, 33, 34). The presence of a stably bound

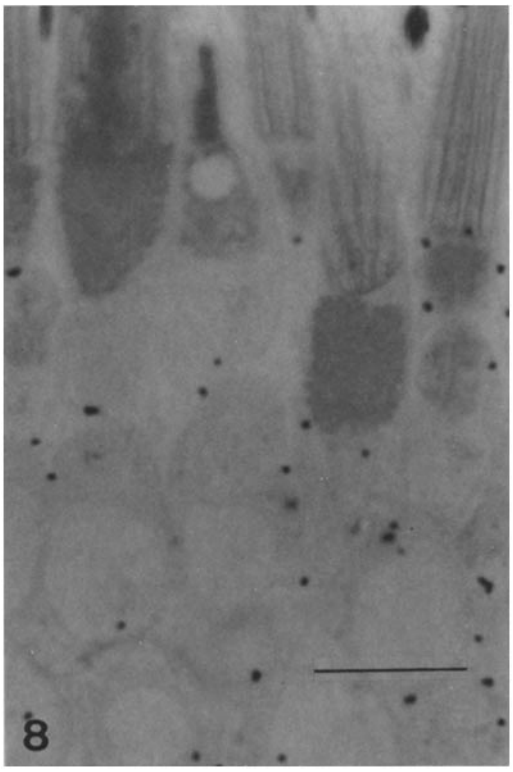

FIGURE 8 [^{3}H]Ouabain autoradiograph prepared from the same animal as in Fig. 6. Experimental conditions were the same except that the incubation medium contained 50×10^{-3} M K^+. Osmolarity was kept constant by decreasing Na^+. Exposure, 16 d; bar, 10 μm.

fraction in 0°C ouabain-free medium (Fig. 1) is consistent with a highly temperature-dependent dissociation rate (2, 33, 34). The high binding affinity ($K_m = 8.3 \times 10^{-8}$ M) for retinal pump sites agrees with the observations of Frank and Goldsmith (14) on ouabain inhibition of frog retinal Na^+,K^+-ATPase ($K_i = 10^{-7}$ M) and those of Mills and colleagues (26) on ouabain binding to frog skin. Furthermore, this agreement shows that extrapolation to equilibrium binding is a reasonable method of estimating the equilibrium binding constant of cardioglycosides in intact tissues. It should be noted that this method is only valid when diffusion rates are fast compared to the association rate (34) and when competing reactions do not limit access to the site of interest (Fig. 12).

The absence of a significant linear uptake component (Fig. 4), the reduction of binding in high K^+ medium (Fig. 8), and the apparent absence of binding at low specific activities (Fig. 9) taken together leave little doubt that nonspecific binding is negligible.

We did not examine the relationship between ouabain concentration and retinal response to light as an additional test of specificity, as this was done by Frank and Goldsmith (14). They observed ~50% inhibition of the electroretinogram (ERG) *b* wave at 10^{-6} M and 30 min of exposure (14, Fig. 2), whereas we observed 60% saturation of binding sites at 0.8×10^{-6} M and 30 min of exposure (Fig. 3). A slight delay between binding and inhibition of the ERG is to be expected, because the ionic gradients must run down for the latter to occur.

Receptor Pump Site Distribution

The major problem that this study set out to solve was how Na^+,K^+ pump sites are quantitatively distributed in the photoreceptor layer. The

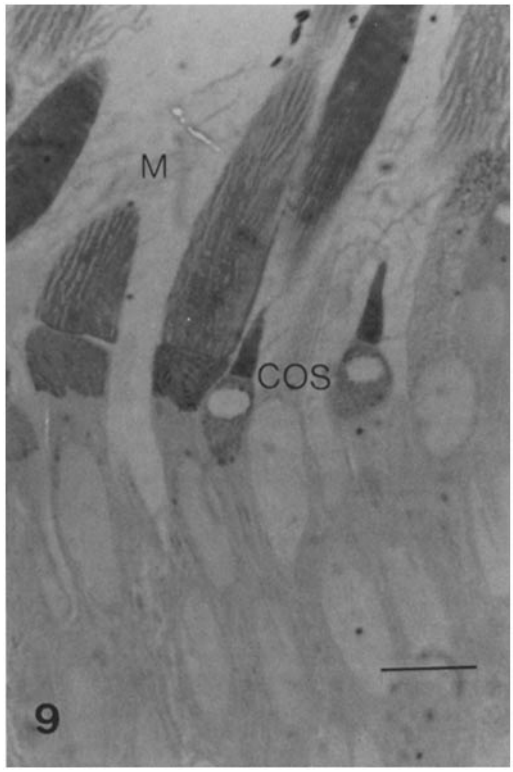

FIGURE 9 An autoradiograph of retina from the same animal as in Fig. 6, incubated for 15 min in 10^{-3} M [^{3}H]ouabain (12.5 μCi/ml) and washed for 20 min. Preservation of cone outer segments (*COS*) was quite good. The grain density over the cells does not differ significantly from that of the wash medium (*M*). Exposure, 8 d; bar, 10 μm.

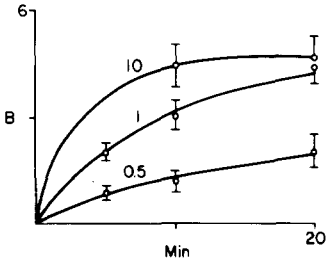

FIGURE 10 Autoradiographic measurement of kinetics in the proximal receptor. Binding (B) is in units of $\times 10^{-6}$ M; the numbers above each curve refer to ouabain concentration $\times 10^{-6}$ M. The curves were determined as in Fig. 3. Each point is the average ± SE bar of six tissue-to-medium grain-density ratios; each tissue area was $\geq 10^3$ μm^2. Radioactive ouabain (μCi/ml) was kept in the range reported for Fig. 2. Autoradiographic exposure varied from 15 to 45 d.

results in Fig. 11 answer this question at the micrometer level. Clearly, there are many more (>90%) pump sites in the proximal layers than in the rod outer segments. It is also equally clear that the modest outer segment binding is specific, for no such binding was observed under high K^+ and with high glycoside concentrations.

The origin of the outer segment sites is certainly a question of interest. Because of light microscope resolution limits, the possibility cannot be excluded that ouabain binds to the fine calyceal processes of the inner segment that extend a considerable distance within the incisures of the outer segment. Preliminary [^{3}H]ouabain autoradiography at the electron microscope level (5) indicates that bullfrog calyces bind ouabain. If, on the other hand, some of the binding sites are located on the outer segment membrane, did they arrive there by diffusion or by a directed process, as in the case of rhodopsin (42)? That binding is most dense at the ciliary junction and declines to zero near the tip suggests diffusion. However, membrane protein diffusion rates (24, 28) are much too rapid compared to outer-segment renewal time (6 wk, 43) to account for the marked gradient of binding shown in Fig. 11. Whatever their origin, their presence could account for the reports (6, 13, 21) of Na^+,K^+-ATPase activity in isolated outer segments.

These observations raise yet another question of basic interest: how the photoreceptor directs Na^+,K^+-ATPase to the proximal layer and rhodopsin to the outer segment. This problem is related to that of epithelia where, for example, in the small intestine Na^+,K^+-ATPase is directed to the basolateral membrane (36), whereas sugar transport sites are directed to the microvillar membranes (39). In the latter case, the tight junction may segregate these two kinds of transport sites. It is not clear how this segregation is effected in photoreceptors.

It is also apparent from Figs. 5 and 10 that Na^+,K^+ pump sites are not distributed uniformly within the proximal half of the receptor layer, as several peaks and valleys of activity were observed. The results in Fig. 11 should be interpreted with caution, as all regions of the retina may not show this precise grain-density distribution. The measurements were derived from a population of ~60 adjacent cells and may be peculiar to the region of the retina analyzed. Nevertheless, we invariably observed a sharp rise in activity at the ciliary junction and an abrupt decline beyond the outer plexiform layer. A major point to be garnered from this analysis is that the pockets of high activity seen in the proximal receptor are real and not the result of random variations in grain density. They may be a consequence of an increase in specific density (number per square micrometer of membrane) or simply a local increase in membrane area. The answer awaits a higher-resolution, quantitative method of localizing these pump sites.

Na^+ Pump Site Density and Cycle Rate

Assuming that each pump site or enzyme binds one molecule of cardioglycoside and that nonreceptor binding in this layer is negligible, the number of pumps per rod is given by Avogadro's number times the ratio of the maximum binding concentration (4.6×10^{-6} M) to the volume of the proximal half of a single receptor (~4,700 μm^3). This calculation yields the value of 13×10^6 sites/rod, especially impressive when compared with the human erythrocyte, which possesses ~200 pump sites. Comparable densities have been reported for epithelial cells (22, 26, 30, 34, 37), which also produce large active Na^+ fluxes.

From the molecular point of view, it is desirable to know the cycling rate of the pump. Zuckerman (44) has estimated from current measurements that about 1.5×10^8 Na^+ ions flow into a frog rod outer segment each second. If, as in the erythrocyte (29) and squid axon (11), three Na^+ ions are pumped out and two K^+ ions are pumped in per cycle, then the cycle rate for an inner-segment pump would be about 4/s. This value agrees reasonably well with calculations (unpublished observations from

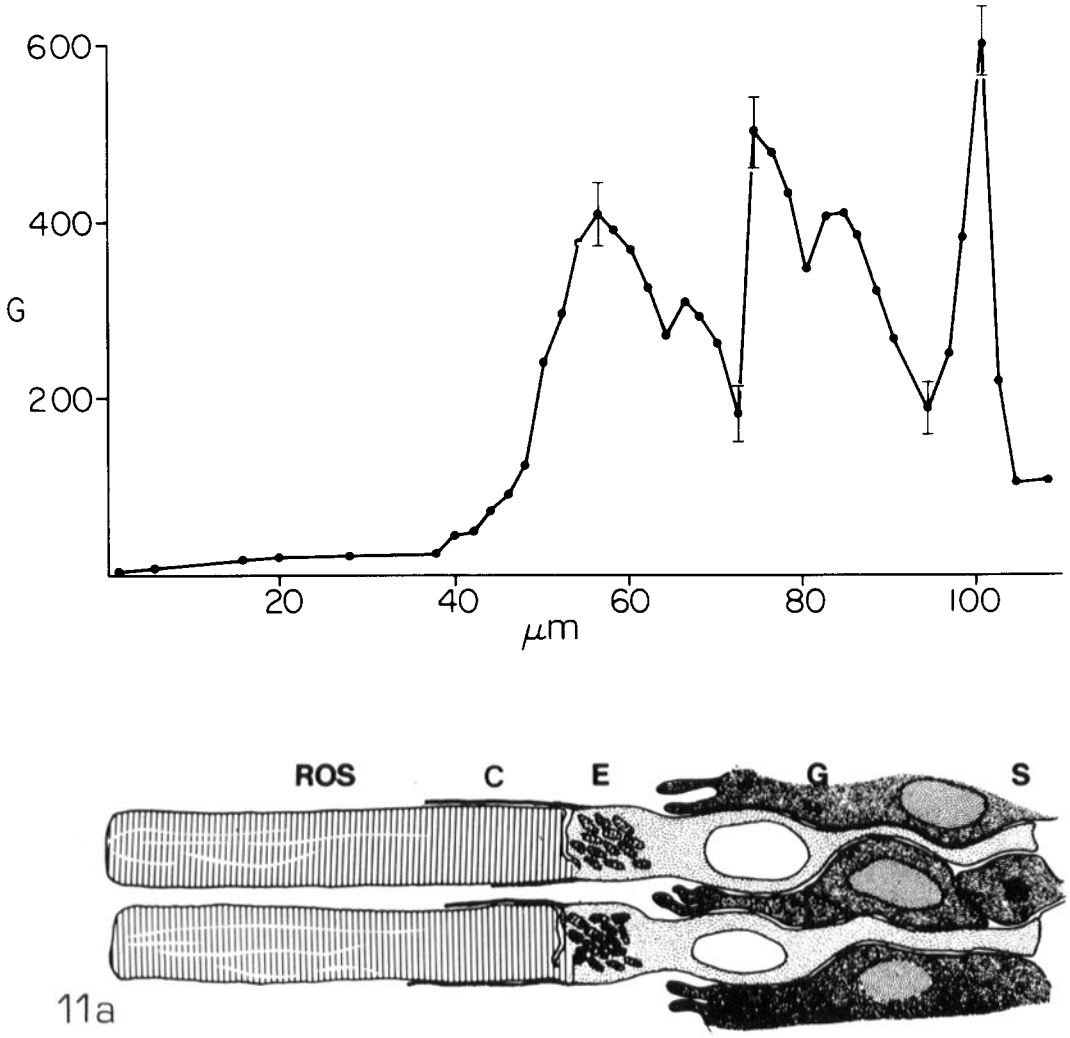

FIGURE 11a Autoradiographic analysis of binding within the photoreceptor layer of retina incubated for 20 min in 10^{-5} M [^{3}H]ouabain and washed for 30 min. Grain density (G) is in grains/10^3 μm^2; distance (μm) is in micrometers. The symbols in the receptor diagram are as in Fig. 5; C, calyceal process. Each point is the mean of five measurements. Except at selected points, SE bars were omitted so as not to clutter the graph.

this laboratory) for other frog cells of 9/s in sartorius muscle and 77/s in skin epithelial cells. A slightly higher cycle rate (27/s) is obtained if the sodium flux estimate (10^9 ions/s × rod) of Korenbrot and Cone (23) is used. In the above calculations the small contribution of cones to the receptor layer has been ignored.

Other Layers

Both the inner plexiform and optic nerve layers exhibited high binding activities. Measurements were not made of the latter. The preliminary data of Fig. 12 suggest that the pump site content of this layer is nearly twice that of the receptor layer. Observations on the retinal epithelium were not presented, as these were ambiguous. In several instances, clumps of the retinal epithelial cells remained loosely attached to the outer-segment layer. We occasionally saw a low level of binding to the apical surface; however, in other experi-

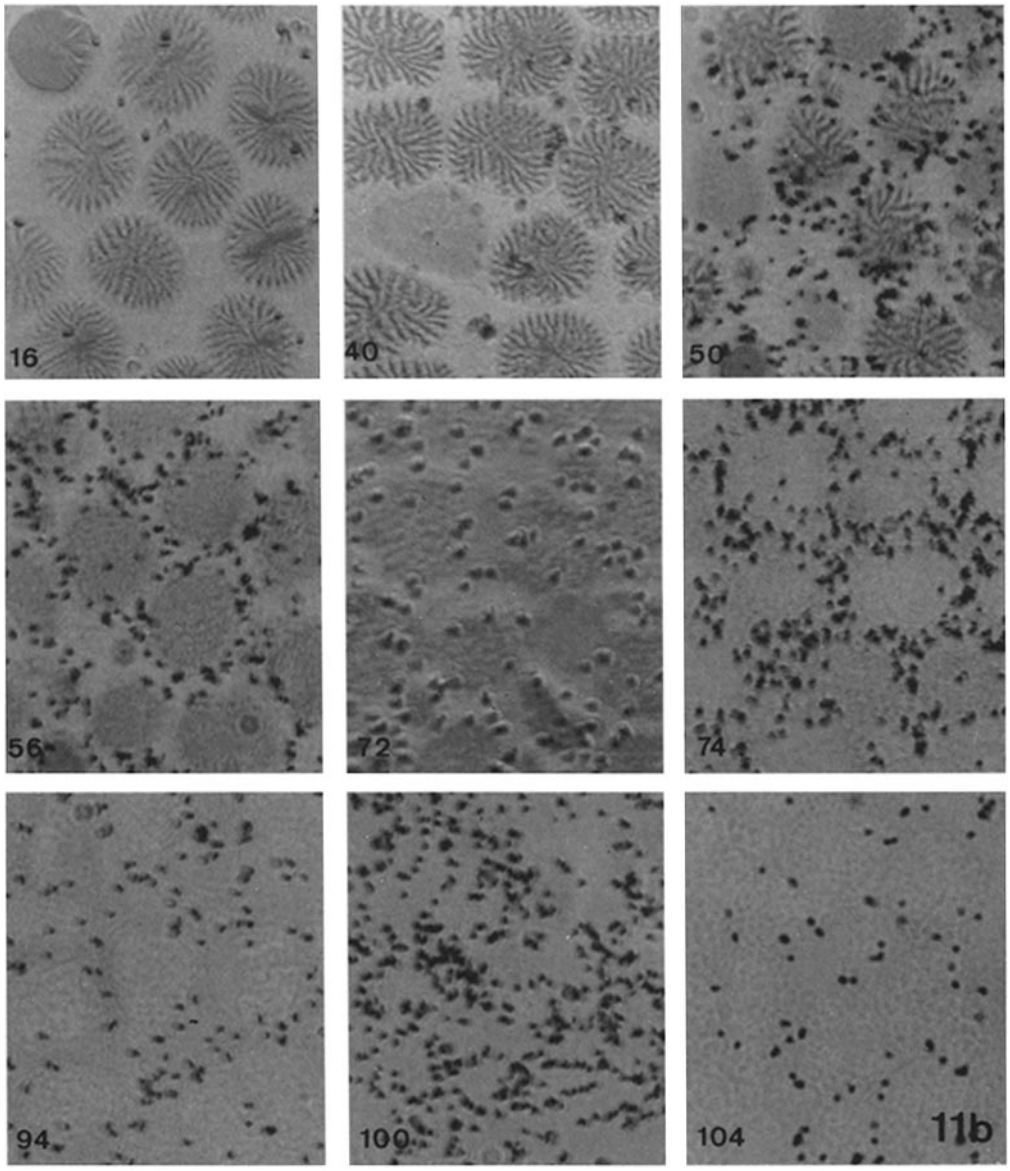

FIGURE 11 b Representative autoradiographs from selected regions of Fig. 11 *a*. Unstained except for OsO_4 fixation. Oblique illumination was used in some to enhance tissue structure. Numbers indicate location (μm) in Fig. 11 *a*. Exposure, 30 d. × 2,000.

ments we did not. Access to the apical surface was not a problem, as the adjacent receptor layer exhibited heavy binding. Silver grain detection at the light microscope level is complicated by the presence of pigmented granules of similar size; hence, we did not pursue this question further. One would expect an apical site of binding from recent studies by Miller et al. (25), and a preliminary report (5) of apical binding was recently published.

Finally, it should be noted that proximal to the outer limiting membrane, the cell type responsible for binding cannot be specified because of resolution limitations. It is doubtful that extension of the present technique to the electron microscope level (5) would answer this question. Perhaps his-

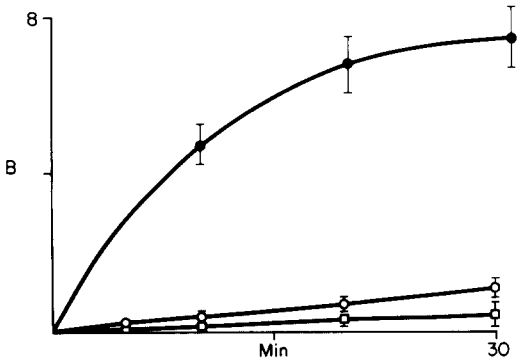

FIGURE 12 Autoradiographic analyses of binding to the inner plexiform layer. Retina was incubated for the indicated times in 10 (●), 1 (○), and 0.5 (□) × 10^{-6} M ouabain. Binding (B) × 10^{-6} M. Each point is based on the mean ± SE of six tissue-to-medium grain-density ratios (each tissue area ≥10^3 μm^2).

tochemical or immunocytochemical techniques will provide this answer.

The authors express their appreciation to Drs. Bunt, Rodieck, and Saari and Mr. Weinberg for their helpful comments.

This study was supported by Public Health Service grants EY-02393 and AM-13183.

Preliminary results of these studies were reported (38) at the 1977 Biophysical Society meetings.

Received for publication 3 August 1979, and in revised form 2 January 1980.

REFERENCES

1. AMES, A., and F. B. NESBETT. 1966. Intracellular and extracellular compartments of mammalian central nervous tissue. *J. Physiol. (Lond.).* **184:**215–238.
2. BAKER, P. F., and J. S. WILLIS. 1972. Binding of the cardiac glycoside ouabain in intact cells. *J. Physiol. (Lond.).* **224:**441–462.
3. BAYLOR, D. A., and M. G. F. FUORTES. 1970. Electrical responses of single cones in the retina of the turtle. *J. Physiol. (Lond.).* **207:**77–92.
4. BERMAN, A. L., A. M. AZIMOVA, and F. G. GRIBAKIN. 1977. Localization of Na^+,K^+-ATPase and Ca^{2+}-activated Mg^{2+}-dependent ATPase in retinal rods. *Vision Res.* **17:**527–535.
5. BOK, D., and B. FILERMAN. 1979. Localization of Na^+,K^+ ATPase in retinal photoreceptors and RPE with ^{3}H-ouabain. *A.R.V.O. (Assoc. Res. Vis. Ophthalmol.)* **18:**224 (Abstr.).
6. BONTING, S. L., L. L. CARAVAGGIO, and M. R. CANADY. 1964. Studies on sodium-potassium-activated adenosine triphosphatase X. Occurrence in retinal rods and relation to rhodopsin. *Exp. Eye Res.* **3:**47–56.
7. BORTOFF, A., and A. L. NORTON. 1967. An electrical model of the vertebrate photoreceptor cell. *Vision Res.* **7:**253–263.
8. BOWNDS, D., A. BRODIE, W. E. ROBINSON, D. PALMER, J. MILLER, and A. SHEDLOVSKY. 1974. Physiology and enzymology of frog photoreceptor membranes. *Exp. Eye Res.* **18:**253–269.
9. BRADFORD, M. 1976. A rapid and sensitive method for quantitation of protein utilizing the principle of protein-dye binding. *Anal. Biochem.* **72:**248–251.
10. BRODERSON, S. H., D. L. PATTON, and W. L. STAHL. 1978. Fine structural localization of potassium-stimulated *p*-nitrophenylphosphatase activity in dendrites of the cerebral cortex. *J. Cell Biol.* **77:**R13–17.
11. CALDWELL, P. C. 1968. Factors governing movement and distribution of inorganic ions in nerve and muscle. *Physiol. Rev.* **48,**1–64.
12. ERNST, S. A., and J. W. MILLS. 1977. Basolateral plasma membrane localization of ouabain-sensitive sodium transport sites in the secretory epithelium of the avian salt gland. *J. Cell Biol.* **75:**74–94.
13. FRANK, R. N., and T. H. GOLDSMITH. 1965. Adenosine triphosphatase activity in the rod outer segments of the pig's retina. *Arch. Biochem. Biophys.* **110:**517–525.
14. FRANK, R. N., and T. H. GOLDSMITH. 1967. Effects of cardiac glycosidase on electrical activity in the isolated retina of the frog. *J. Gen. Physiol.* **50:**1585–1606.
15. FUORTES, M. G. F., and A. L. HODGKIN. 1964. Changes in time scale and sensitivity in the ommatidia of *Limulus*. *J. Physiol. (Lond.).* **172:** 239–263.
16. FUORTES, M. G. F., and P. M. O'BRYAN. 1972. Generator potentials in invertebrate photoreceptors. *In* Handbook of Sensory Physiology, Vol. VII/2. Springer-Verlag, Berlin. 279–319.
17. GRANDA, A. M., and C. A. DVORAK. 1977. Vision in turtles. *In* Handbook of Sensory Physiology, Vol. VII/5. Springer-Verlag, Berlin. 451–492.
18. HAGINS, W. A. 1972. The visual process: excitatory mechanisms in the primary receptor cells. *Annu. Rev. Biophys. Bioeng.* **1:**131–154.
19. HAGINS, W. A., R. D. PENN, and S. YOSHIKAMI. 1970. Dark current and photocurrent in retinal rods. *Biophys. J.* **10:**380–412.
20. HAGINS, W. A., W. E. ROBINSON, and S. YOSHIKAMI. 1975. Ionic aspects of excitation in rod outer segments. *In* Energy Transformation in Biological Systems. CIBA Found. Symp. **31:**169–189.
21. HEMMINKI, K. 1975. Localization of ATPase in bovine retinal outer segments. *Exp. Eye Res.* **20:**79–88.
22. KARNAKY, K. J., L. B. KINTER, W. B. KINTER, and C. E. STIRLING. 1976. Teleost chloride cell. II. Autoradiographic localization of Na,K-ATPase in killifish *Fundulus heteroclitus* adapted to low and high salinity environments. *J. Cell Biol.* **70:**157–177.
23. KORENBROT, J. I., and R. A. CONE. 1972. Dark ionic flux and the effects of light in isolated rod outer segments. *J. Gen. Physiol.* **60:**20–45.
24. LIEBMAN, P. A., and G. ENTINE. 1974. Lateral diffusion of visual pigments in photoreceptor disc membranes. *Science (Wash. D.C.).* **185:** 457–459.
25. MILLER, S. S., R. STEINBERG, and B. OAKLEY III. 1978. *J. Membr. Biol.* **44:**259–279.
26. MILLS, J. S., S. A. ERNST, and D. DIBONA. 1977. Localization of Na^+ pump sites in frog skin. *J. Cell Biol.* **73:**88–110.
27. NILSSON, S. E. G. 1964. An electron microscope classification of the retinal receptors of the leopard frog (*Rana pipiens*). *J. Ultrastruct. Res.* **10:**390–416.
28. POO, M., and R. A. CONE. 1974. Lateral diffusion of rhodopsin in the photoreceptor membrane. *Nature (Lond.).* **247:**438–441.
29. POST, R. L. and P. C. JOLLY. 1957. The linkage of sodium, potassium and ammonium active transport across the human erythrocyte membrane. *Biochim. Biophys. Acta.* **25:**118–128.
30. QUINTON, P. M., E. M. WRIGHT, and J. MCD. TORMEY. 1973. Localization of sodium pumps in the choroid plexus epithelium. *J. Cell Biol.* **58:**724–730.
31. RICHARDSON, K. D., L. JARRETT, and E. H. FINKE. 1960. Embedding in epoxy resins for ultrathin sectioning in electron microscopy. *Stain Technol.* **35:**313–323.
32. RODIECK, R. W. 1973. The Vertebrate Retina. W. H. Freeman & Company, San Francisco. 296–337.
33. SCHWARTZ, A., G. E. LINDEMAYER, and J. C. ALLEN. 1975. The sodium-potassium adenosine triphosphatase; pharmacological, physiological and biochemical aspects. *Pharmacol. Rev.* **27:**1–134.
34. SHAVER, J. L. F., and C. E. STIRLING. 1978. Ouabain binding to renal tubules of the rabbit. *J. Cell Biol.* **76:**278–292.
35. STAHL, W. L., and S. H. BRODERSON. 1976. Localization of Na^+,K^+-ATPase in brain. *Fed. Proc.* **35:**1260–1265.
36. STIRLING, C. E. 1972. Radioautographic localization of sodium pump sites in rabbit intestine. *J. Cell Biol.* **53:**704–714.
37. STIRLING, C. E. 1976. High resolution autoradiography of ^{3}H-ouabain binding in salt transporting epithelia. *J. Microsc. (Oxf.).* **106:**145–157.
38. STIRLING, C. E. 1977. ^{3}H-ouabain binding to frog retina. *Biophys. J.* **17:** 196*a*.
39. STIRLING, C. E., and W. B. KINTER. 1967. High-resolution radioautography of galactose-^{3}H accumulation in rings of hamster intestine. *J. Cell Biol.* **35:**585–604.
40. TOMITA, T. 1972. Light-induced potential and resistance changes in vertebrate photoreceptors. *In* Handbook of Sensory Physiology, Vol. VII/2. Springer-Verlag, Berlin. 483–511.
41. TOYODA, J., H. NOSAKI, and T. TOMITA. 1969. Light-induced resistance changes in single photoreceptors of *Necturus* and *Gekko*. *Vision Res.* **9:** 453–463.
42. YOSHIKAMI, S., AND W. A. HAGINS. 1973. Control of the dark current in vertebrate rods and cones. *In* Biochemistry and Physiology of Visual Pigments. H. Langer, editor. Springer-Verlag, Heidelberg. 245–255.
43. YOUNG, R. W. 1967. The renewal of photoreceptor cell outer segments. *J. Cell Biol.* **33:**61–72.
44. ZUCKERMAN, R. 1973. Ionic analysis of photoreceptor membrane currents. *J. Physiol. (Lond.).* **235:**333–354.